Jet Circulation Control Airfoil for VTOL Rotors

S. W. YUAN*
George Washington University, Washington, D. C.

Based on the potential flow theory calculation, the capacity of the air supply, the limitation of the internal pressure of the model and the limitation due to the compressibility effect of the jet stream at high velocities, the elliptical airfoils of 18 and 12% thickness ratios were designed and constructed. Experimental investigations for both models with trailing-edge jets include force and pitching moment measurements. In addition, static pressure measurements were made in both spanwise and chordwise directions. These results were used to compare with available theories as well as other experimental data. Circulation control with dual jets for the elliptical airfoil of 18% thickness ratio was tested with very satisfactory results. The determination of the aerodynamic response of the airfoil model to cyclic changes in jet mass flow was also made. The cyclic results were very satisfactory and are presented in the form of pulsating lift coefficient, drag coefficient, and pressure coefficient as a function of pulsating jet coefficient.

Nomenclature

Fluid and flow properties

p = pressure
p_∞ = freestream pressure
Q = $A_J V_J$, volume flow rate of jet, ft³/sec
u = local velocity relative to airfoil
$U_{\max}$ = maximum potential flow velocity (at minimum pressure point)
U_∞ = freestream velocity
V_J = jet fluid velocity relative to airfoil
V_{xJ} = jet induced velocity component in the x direction
ν = kinematic viscosity of air
ρ = freestream air density
ρ_J = jet air density

Geometrical properties

a,b = semiaxes of elliptical airfoil
$2a$ = airfoil chord
A_J = jet slot area
ℓ = span of the airfoil
x,y = rectangular coordinates of the ellipse
$\bar{x}$ = $x/2a$, measured from the leading edge of the airfoil
α = angle of attack
ζ = complex plane ($\zeta = \xi + i\eta$)
θ = jet deflection angle with respect to the chord line
ξ,η = elliptical coordinates (see Fig. 1)
ξ_0 = values of ξ on the ellipse
σ = jet slot width

Forces

D = total drag
J = total jet reaction or momentum flux at the slot $J = \rho_J A_J V_J^2$
L = total lift

Nondimensional coefficient

C_{do} = section drag coefficient
C_J = jet coefficient $C_J = [J/\rho U_\infty^2(2al)]/2 = (\rho_J/\rho) \times (1/A_J al)(Q/U_\infty)^2$
C_L = total lift coefficient $C_L = C_{Lp} + C_J \sin\theta$
C_{L_3} = flat plate loading coefficient defined in Eq. (3)
C_p = pressure coefficient
C_m = pitching moment coefficient (relative to the midchord point)
C_{Lp} = pressure lift coefficient
Re = Reynolds number ($Re = U_\infty 2a/\nu$)

Miscellaneous

k = practical jet shape factor ($k = 1.0$ is assumed in this investigation)
γ = a constant [see Eq. (10)]

Presented as Paper 69-741 at the CASI/AIAA Subsonic Aero- and Hydro-Dynamics Meeting, Ottawa, Canada, July 2-3, 1969; submitted July 22, 1969; revision received January 5, 1970. This research was originally supported by U. S. Army Aviation Material Laboratories, Fort Eustis, Va., under Contract DA-44-177-AMC-200 (T).

* Professor of Engineering and Applied Science. Associate Fellow AIAA.

Introduction

FOR two-dimensional flow of a uniform stream past an airfoil, the Kutta-Joukowski hypothesis states that the strength of circulation about an airfoil will always adjust itself so that the velocity is finite at the trailing edge. Based on this hypothesis, airfoils are designed with sharp trailing edges so that the increase of lift depends entirely on the increase of the angle of attack.

If an airfoil is designed with a trailing edge of finite curvature, the rear stagnation point in the potential flow is not situated at a fixed point. Furthermore, the production of lift in this case is not necessarily dependent on the geometrical angle of attack of the airfoil but depends on the position of the rear stagnation point, which can be artificially fixed. The control of lift for an airfoil with a round trailing edge can be achieved by placing a thin jet issuing from the rear stagnation point at an angle approximately along the calculated rear dividing streamline.

The proposed rotor system consists of rotor blades having a cross-section shape which resembles an ellipse with circulation control by means of jets (through narrow spanwise slots) located beneath the blade airfoil sections. The lifting force that is created by both circulation and jet reaction can be controlled by means of the jet velocity, which in turn can be controlled simply by regulating the mass flow (both cyclically and collectively) from the power source. Hence, this rotor system requires only simple rigidly mounted blades (with fixed blade angle if desired) at the rotor hub. Furthermore, it appears that the use of an airfoil of oval profile can result in lift regardless of forward or rearward flow (leading-edge jet is used) relative to the airfoil, so that there is almost no loss of lift in the reverse flow region experienced at higher forward speeds. As a consequence, the proposed helicopter rotor system could not suffer as great a limitation in forward speed as does an orthodox helicopter. Furthermore, since

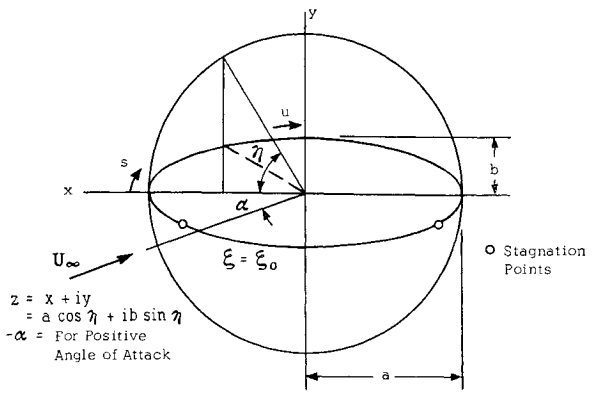

Fig. 1 Elliptical coordinates.

there is no loss of lift in the reverse flow region, stop rotor in flight can be smoothly carried out when the system is applied to the stopped rotor/wing craft.

The purpose of this experimental investigation is to study the basic aerodynamic characteristics of an elliptical airfoil with jet circulation control. Furthermore, exploratory investigations were conducted in order to gain knowledge in the area of a dual-jet system (both leading-and trailing-edge jets) and the aerodynamic response of the elliptical airfoil to rapid cyclic change in jet momentum. It is believed that the results of this study presented here will provide adequate information to justify further investigation toward the application of this type of airfoil system to VTOL rotors.

Theoretical Calculation

For an ellipse, the velocity distribution for the potential flow can be calculated from the known complex potential for a circle with the aid of the transformation between a circle and an ellipse. If the potential flow about the circle consists of a parallel and a circulatory flow, the velocity at any point on the elliptical airfoil, as determined by the aforementioned transformation, can be written as

$$\frac{u}{U_\infty} = \frac{1}{U_\infty}\left|\frac{dF}{dz}\right| = \frac{(1 + b/a)\sin(\eta - \alpha) + C_L/2\pi}{[\sin^2\eta + (b/a)^2\cos^2\eta]^{1/2}} \quad (1)$$

For a given C_L, the coordinates for the dividing streamlines for an elliptical airfoil are obtained as follows:

$$x/a = [\cosh(\xi - \xi_0) + (b/a)\sinh(\xi - \xi_0)] \times (F(\xi)\sin\alpha + \cos\alpha\{1 - [F(\xi)]^2\}^{1/2})$$

$$y/a = [\cosh(\xi - \xi_0) + (a/b)\sinh(\xi - \xi_0)] \times (-F(\xi)\cos\alpha + \sin\alpha\{1 - [F(\xi)]^2\}^{1/2}) \quad (2)$$

where

$$F(\xi) = [(\xi - \xi_0)C_L]/[2\pi(1 + b/a)\sinh(\xi - \xi_0)]$$

The previous nomenclatures are shown in Fig. 1, and the coordinates of the stagnation points can be obtained from Eq. (2) by putting $\xi = \xi_0$.

Equation (1) gives the velocity distribution in the potential flow of an elliptical airfoil with a thin flap placed along the calculated rear dividing streamline. It is assumed that there is no separation of flow in the boundary layer.

If a jet is established at the calculated rear stagnation point and ejected at high velocity along the rear dividing streamline, the additional energy imparted to the boundary layer may overcome the wall friction and prevent flow separation. Furthermore, the jet may produce a "supercirculation" above the circulation necessary to keep the flow attached if the momentum of the jet is sufficiently large and separations of flow do not occur.

An approximate method for calculating the pressure distribution of a two-dimensional airfoil in inviscid incompressible flow with jet issuing from the lower surface near the trailing edge was investigated by Weber[1] and Küchemann.[2] According to the method given by Weber,[1] the pressure coefficient of elliptical airfoils is calculated in the form

$$C_p = 1 - \left[1/1 + \left(\frac{b}{a}\right)^2 \frac{(1 - 2\bar{x})^2}{1 - (1 - 2\bar{x})^2}\right] \times \left[\left(1 + \frac{b}{a} + \frac{V_{xJ}}{U_\infty}\right)\cos\alpha \pm \left\{\left(\frac{C_{Lp} + C_{L3}}{4\pi} + \sin\alpha\right) \times \left(\frac{1 - \bar{x}}{\bar{x}}\right)^{1/2} + \frac{C_{Lp} - C_{L3}}{4\pi}\left(\frac{\bar{x}}{1 - \bar{x}}\right)^{1/2}\right\}\left(1 + \frac{b}{a}\right)\right]^2 \quad (3)$$

where the jet-induced velocity component parallel to the chord

$$V_{xJ}/U_\infty = 0.005[(aC_J/\sigma)^{1/2} - 1]$$

and

$$C_{L3} = 2\pi(C_J/C_{Lp})(1 - \cos\theta)$$

Equation (3) may be used to calculate the pressure distribution for an elliptical airfoil with trailing-edge jet at any given C_{Lp}, provided the C_{Lp} and C_J relation is known. For a thin airfoil (12.5% thickness ratio and less), the relation between C_{Lp} and C_J is given by[3]

$$C_{Lp}/\theta = 3.54C_J^{1/2} - 0.675C_J + 0.156C_J^{3/2} \quad (4)$$

However, for the elliptical airfoil of 18% thickness ratio, the previous expression does not give accurate results, and approximate estimation of C_{Lp} and C_J must be made.

Description of Experiment

Model

Based on the theoretical results obtained in the previous section, the capacity of the air supply, the limitation of the internal pressure of the model, and the limitation due to the compressibility effect of the jet stream at high velocity, the elliptical airfoil of 18% thickness ratio was designed first and subsequently the 12% model. According to the model geometrical configuration, the expression for C_J is

$$C_J = 135.7(Q/U_\infty)^2 \quad (5)$$

for the 18% model and

$$C_J = 121.6(Q/U_\infty)^2 \quad (6)$$

for the 12% model. The average value of Q corresponding to 6-in. pressure inside the model is 2.5 ft^4/sec for 18% elliptical airfoil and 3.37 ft^3/sec for 12% airfoil.

For a given value of volume flow rate of jet Q the value of C_J can be determined from Eqs. (5) and (6) which in turn may be used to estimate the values of C_L for both modesl from the following empirical equation[3]:

$$C_L = 2k\sin\theta(2\pi C_J)^{1/2}[1 + (\pi/48)(C_J/k^2) + \ldots] \quad (7)$$

For example, $C_J = 0.5$, $k = 1$ for the 18% model, the estimated total lift coefficient is $C_L = 1.83$, and the corresponding test result gives $C_L = 2.05$ (Fig. 7).

The 18% thickness elliptical model has a 12-in. chord and a 36.5-in. span. As seen in Fig. 2, the main structural member is a $1\frac{3}{8}$-in. o. d., round steel tube which also supplied the air for the jet. The trailing-edge jet slot width is 0.019 ± 0.001 in. wide, at an angle of 30° to the model chord plane. Seventy-six static pressure taps were installed spanwise along the top and bottom surfaces at the 50% chord line and, similarly, 47 taps in the chordwise direction in the midspan plane.

The blowing air entered the interior of the model through 11 pairs of diametrically opposed slots in the steel support

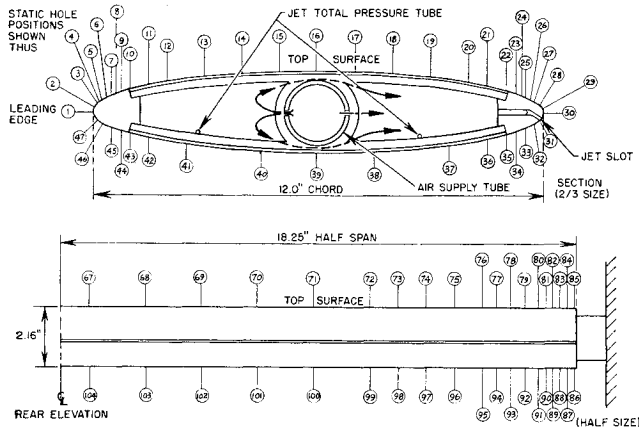

Fig. 2 Section of model showing locations of the static pressure taps (18% thickness ratio).

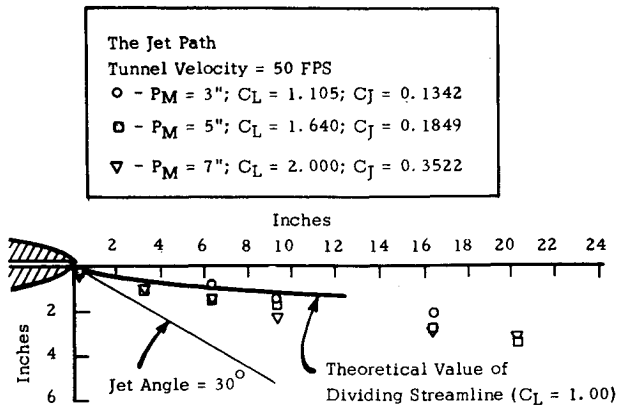

Fig. 3 Dividing streamline and jet path for elliptical airfoil of 18% thickness ratio.

tube, and exhausted in the chord direction. The support tube was clamped on one end to a stand outside the tunnel; thus, the model was mounted horizontally in the test section, cantilevered from one end. After the first model was tested with the trailing-edge jet only, it was dismantled and a new leading edge was installed having a slot 0.03 ± 0.001 in. wide also at an angle of 30° to the chord plane. A multiple-gate type valve was installed to control the air flow to the forward jet.

The construction of the 12% thickness elliptical model is essentially the same as described previously for the 18% thickness model. However, this model has a jet-slot width of 0.023 ± 0.001 in. and the jet is at an angle of 40° to the chord line.

Auxiliary Air Supply

An auxiliary air supply that was used to provide jet blowing of the model consisted of a series of storage tanks having a total volume of 200 ft³. These tanks were supplied constantly by the main compressed air supply system at 100-lb gage pressure. The air was routed to the tunnel test section through $2\frac{1}{2}$-in. pipe containing two manually controlled valves and an orifice-plate flowmeter. The orifice meter was used to obtain a correlation between mass flow rate and model internal pressure for each slot configuration. This permitted the determination of flow rates from the measured model pressure, rather than using the more cumbersome orifice.

In order to determine the aerodynamic response of the model to cyclic changes in blowing, a series of dynamic tests were made. A butterfly-type valve was installed in the air supply tube of the 18% thickness model. The valve was designed so that it could be continuously rotated at any desired rate by means of a motor connected to the valve shaft. The rotating valve produced a pulsating pressure in the model that in turn resulted in cyclic flow of the jet. The flow cycle was that of a sinusoidal wave.

Wind Tunnel

The tests were conducted in the subsonic wind tunnel of the University of Texas.[4] The tunnel is of the continuous-flow, closed-circuit type, capable of a maximum velocity of 175 fps. The closed test section is 38 in. long, and all four walls diverge to compensate for boundary-layer thickening. The entrance is approximately 22 in. high and 36 in. wide; the exit is 26 in. by 39 in. The test section static pressure is essentially atmospheric for all tests.

Force Measurements

The model was mounted as a cantilevered beam by clamping the support tube to a stand fixed to the building floor. Strain gages were mounted on the tube between the clamps and the tunnel wall; three bridges were installed, oriented to measure lift, drag and pitching moment. The outputs were manually recorded using SR-4 strain indicators. The pitching moments proved to be too small to measure with reasonable accuracy.

The 14-channel Midwestern Instrument 621 oscillograph was used to record the model forces for the dynamic tests during which the blowing rate was varied. The output of the strain gage bridges was too low to permit recording on the oscillograph; hence, linear variable differential transformers were mounted at the free end of the model to measure the deflections due to lift and drag. A calibration between the forces and resulting deflections was made using dead weights and pulleys.

Pressure Measurements

The steady-state pressure measurements were made using multiple-tube manometer boards filled with oil at 0.9 specific gravity. The manometer readings were manually recorded.

The measurement of the model surface static pressures during the dynamic tests was made using five Pace Model P7D-±1.0 psig variable-reluctance type pressure transducers. These were mounted outside the wind-tunnel wall and connected to various chordwise pressure orifices using plastic tubing installed inside the 12% thickness ratio model. One transducer was connected to measure the model internal (blowing) pressure. The transducer output was rectified and recorded on an oscillograph. The transducers were selected because of their low internal volume and high natural frequency.

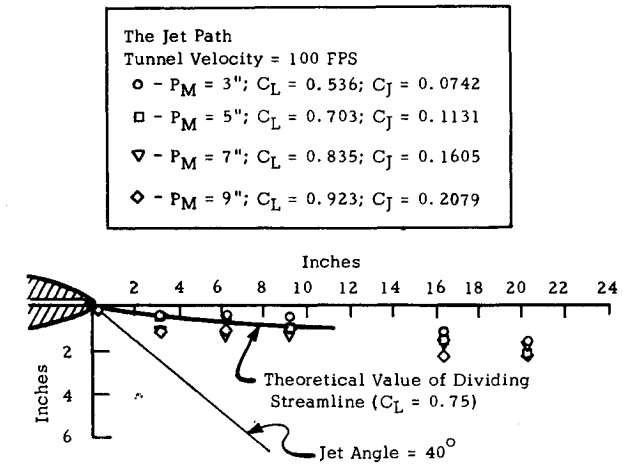

Fig. 4 Dividing streamline and jet path for elliptical airfoil of 12% thickness ratio.

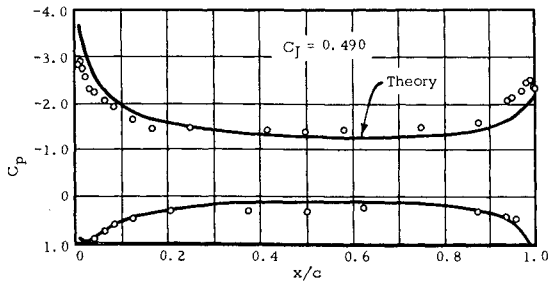

Fig. 5 Pressure distribution in the chordwise direction for the elliptical airfoil of 18% thickness ratio.

Results and Discussion

Shape of the Jet

Measurements of the shape of the jet were made at six stations between $\frac{1}{8}$ in. and $20\frac{1}{8}$ in. behind the trailing-edge jet slot. Pitot tubes were carefully aligned in order to locate the position of maximum total pressure in any one plane. Experiments were made using both models at different wind-tunnel velocities and several different mass flow rates of the jet for each tunnel velocity.

The results of the previously described data were reduced to the single parameter C_J, jet coefficient. With these C_J values, any desired lift coefficient can be determined from the C_L vs C_J curves. The theoretical and experimental results for both models are shown in Fig. 3 for the elliptical airfoil of 18% thickness ratio and in Fig. 4 for the 12% thickness ratio. In each case the agreement is reasonably good.

Pressure Distribution

The results of the tests show that the spanwise pressure distribution for each of the models is very nearly constant, which can be said that a two-dimensional investigation is fulfilled. A typical pressure distribution curve in the chordwise direction for each of the models is shown in Fig. 5 and Fig. 6, respectively. It is seen that the comparisons between the measured pressure distributions and the corresponding theoretically calculated values are considered to be in reasonably good agreement.

The integration of the static pressures over the chord gives the pressure lift force per unit span. The results of the integration of the pressure distribution curves, after reducing to pressure lift coefficient C_{Lp}, are shown in Fig. 7. The agreement between the results of C_{Lp} from the pressure measurement and those from direct total lift measurement [see Eq. (8)] is considered to be good.

Lift

The lift forces at zero angle of attack were measured for both models at various wind-tunnel velocities ($1.5 \times 10^5 \leqslant Re \leqslant 9 \times 10^5$) and trailing-edge jet velocities. The data were reduced to coefficient forms and plotted as total lift coefficient vs jet coefficient. In Fig. 7, the total lift coefficient is shown as a function of the jet coefficient C_J for the elliptical airfoil of 18% thickness ratio.

The pressure lift coefficient C_{Lp} is defined as

$$C_L = C_{Lp} + C_J \sin\theta \tag{8}$$

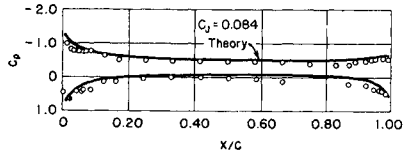

Fig. 6 Pressure distribution in the chordwise direction for the elliptical airfoil of 12% thickness ratio.

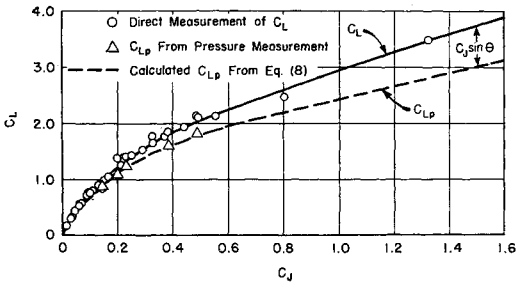

Fig. 7 Lift coefficient vs jet coefficient for elliptical airfoil of 18% thickness ratio (θ = 30°, α = 0).

and the curve of C_{Lp} against C_J as calculated from Eq. (8) is also shown in Fig. 7. The values of the pressure lift coefficient C_{Lp} are also calculated from the measured static pressure on the surface of the model, and these values are shown in Fig. 7. These measured values of C_{Lp} agree very well with those obtained from Eq. (8).

The total lift forces for the elliptical airfoil of 18% thickness ratio was also measured at different angles of attack. The total lift coefficient vs the angle of attack with jet coefficient as a parameter is shown in Fig. 8. With the jet coefficient $C_J < 1.0$, the total lift coefficient at small angles of attack can be expressed by the following equations[3]:

$$C_L = C_{L\alpha=0} + \alpha(\partial C_L/\partial\alpha)_{\alpha=0} \tag{9}$$

where

$$\left(\frac{\partial C_L}{\partial\alpha}\right)_{\alpha=0} = 2\pi\left[1 + \frac{k}{(2\pi)^{1/2}} C_J^{1/2} + \frac{\pi}{24k} C_J + \frac{1}{24\pi k}\left(\frac{\pi C_J}{2}\right)^{3/2} + \cdots\right]$$

As a typical example, when $C_J = 0.4$ and $\alpha = 4°$, the calculated value of C_L from Eq. (9) is $C_L = 2.57$ and the corresponding measured value is $C_L = 2.45$. The difference between the calculated and experimental values is within 5%.

From Fig. 8, it may be seen that the stalling point occurs at an angle of attack of 5° for $C_J = 1.2$; however, it may also be noted that the stalling point occurs at higher angles of attack as the value of C_J decreases. The decrease of C_L after the stalling point for the elliptical airfoil with trailing-edge jet is rather gradual in contrast to the sharp drop of C_L for the convention airfoil.

In order to compare the present results with those obtained in the NGTE[5] a plot of total lift coefficient vs jet coefficient parameter $C_J \sin\theta$ for elliptical airfoils of 12 and $12\frac{1}{2}$% thickness ratio, respectively, is shown in Fig. 9. The

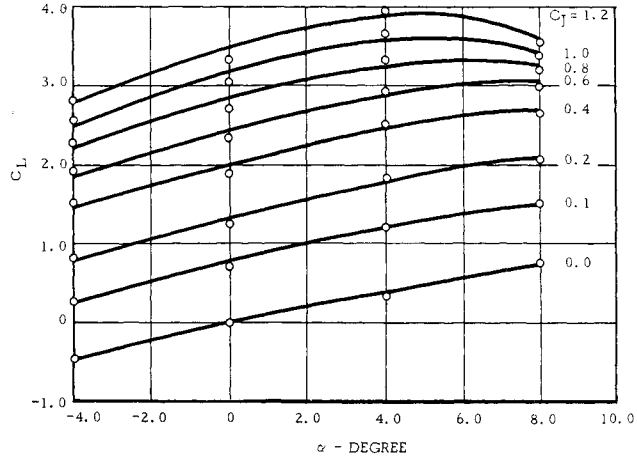

Fig. 8 Total lift coefficient vs angle of attack at various values of C_J (b/a = 18%).

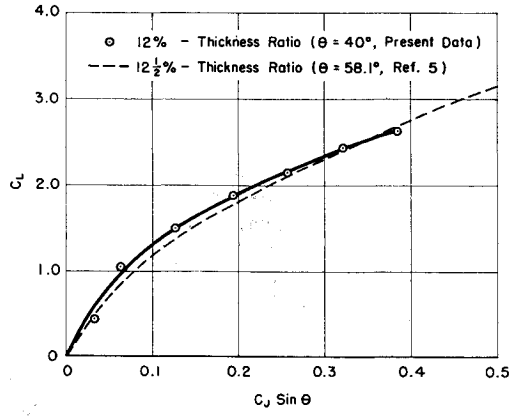

Fig. 9 Lift coefficient vs jet coefficient parameter for elliptical airfoils.

agreement between these two sets of measurement data is considered to be very good even though the data obtained by the NGTE was based on jet deflection angle of 58.1°. The previously results confirm the validity of the empirical relation given in Eq. (7).

Drag

According to thrust hypothesis[6] for an idealized jet flap system, the total thrust experienced by the airfoil model is equal to the total jet reaction disregarding the angle of deflection of the jet. This hypothesis is based on the assumption that no mixing occurs between the main stream and the jet and that no separations of flows appear. Actually, however, the measured thrust (negative drag) is less than the ideal system predicted. This discrepancy occurs since there is a loss in the mixing process between the main stream and the jet sheet as well as the existence of frictional drag.

Figure 10 depicts a comparison of section drag coefficient vs lift coefficient between the elliptical airfoil of 12% thickness ratio and the NACA 0012 airfoil. The data of the NACA 0012 airfoils are taken from NACA TR 460 and the results of the elliptical airfoil are calculated from the present data.[4] The section drag coefficient of the elliptical airfoil is obtained by taking the difference of the measured values of the jet thrust coefficient and the corresponding calculated values (correction for $Re = 3.23 \times 10^6$ was made). Since the measured values of the jet drag (Fig. 36 of Ref. 4) of the elliptical airfoil consist of both jet reaction and frictional drag whereas the calculated values are merely the jet reaction, the difference of these two sets of values gives the section drag of the airfoil. The results indicate that the section drag coefficient of the elliptical airfoil is smaller than that of NACA section particularly for lift coefficients beyond $C_L = 1.3$.

Pitching Moment

The pitching moment on the elliptical airfoil was found by the combination of the results of a graphical integration of the

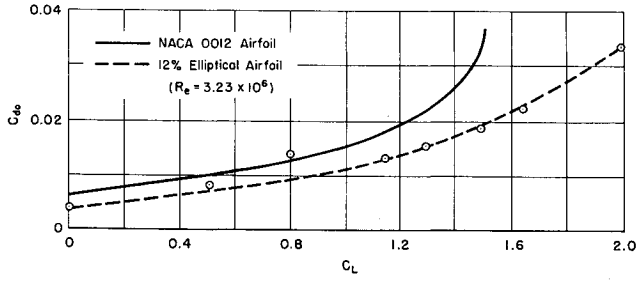

Fig. 10 Comparison of section drag coefficient.

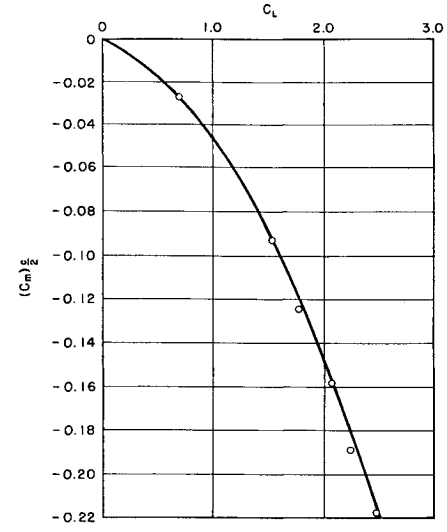

Fig. 11 Pitching moment coefficient vs lift coefficient (relative to midchord point) for model of 12% thickness ratio.

moment of area of the pressure distribution curve about the midchord point with the moment due to the jet reaction. The position of the center of lift can be obtained from the pitching moment and lift coefficient data. Figure 11 shows the variation of the pitching moment coefficient C_m with total lift coefficient C_L for the models of 18% thickness ratios.

According to the experimental data (Fig. 11), the pitching moment coefficient can be expressed as a function of C_L and C_J in the following form:

$$C_m = (C_L/4) - \gamma C_J^{1/2}(C_L + 2\pi) \qquad (10)$$

where γ is a constant depending on the airfoil geometry and the jet angle. For the elliptical airfoil of 12% model ($\theta = 40°$), the values of γ are between 0.105 to 0.12 for $0.05 \leq C_J \leq 0.40$.

Dual Jets

If the potential flow is calculated about an elliptical airfoil corresponding to an arbitrary circulation, the two symmetrical dividing streamlines are known and a certain lift is obtained. According to the results discussed previously, it is seen that a lift of a desired magnitude would be produced if a jet stream was placed along the calculated rear dividing streamline of the elliptical airfoil corresponding to a specific circulation.

Now suppose that the two jet streams ejecting outward were placed along the two dividing streamlines of the elliptical airfoil in a wind tunnel. This exploratory experiment was performed on the elliptical airfoil of 18% thickness ratio with dual jets, symmetrically located as described previously. The tests were made, at Reynolds number $Re = 5.5 \times 10^5$, by

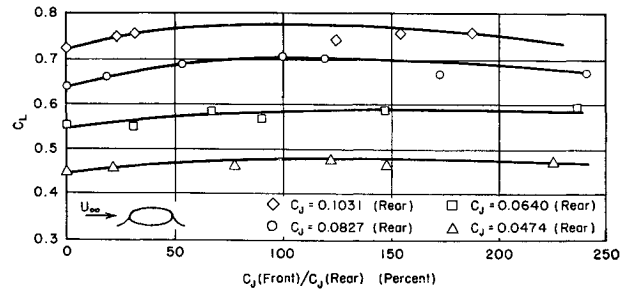

Fig. 12 Total lift coefficient vs ratio of leading-edge jet coefficient to trailing-edge jet coefficient (18% thickness ratio).

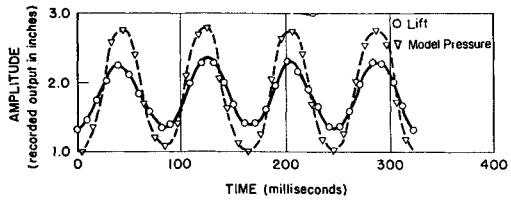

Fig. 13 Pulsating lift and model pressure for elliptical airfoil of 18% thickness ratio (valve speed = 360 rpm).

varying the mass flow of the leading-edge jet while the mass flow of the trailing-edge jet was maintained constant. The results of this test are presented in Fig. 12 and show the variation of the total lift coefficient as a function of the ratio of the leading edge C_J to the trailing edge C_J, $(C_J)_F/(C_J)_R$. For $(C_J)_F/(C_J)_R = 0$, the total lift coefficient is equal to the case of airfoil with trailing-edge jet only. As the mass flow of the leading jet increases from zero value, the total lift increases gradually. This increase of total lift is equivalent to the reaction resulting from the front jet. It is very interesting to note that even though the mass flow of the leading-edge jet exceeds that of the rear jet by 50%, the total lift still remains above its original value when $(C_J)_F = 0$.

The important application of the elliptical airfoil (or any oval airfoil) with dual jets to the retreating blade of a rotor is evident. At high transverse speeds of a rotor, a sizable portion of the retreating blade experiences a reversal of relative airflow. This produces a condition of no lift or even a negative lift on a conventional rotor blade. If the elliptical airfoil with dual jets is used for the blade, the loss of lift in the reverse flow region which is experienced in present day rotor systems can be greatly eliminated. In the application of this rotor-blade system to the stopped rotor/wing craft, it can be seen that the rotor blades can be smoothly stopped.

Aerodynamic Response of the Model to Cyclic Change of Jet

In a conventional type of helicopter rotor, the control of the lift coefficient C_L must be effected by a change in incidence or angle of attack of the airfoil. The circulation created in this case is the result of the Kutta flow condition at the sharp trailing edge. In the present study, it is indicated that the value of C_L can be controlled by simply varying mass flow of the jet. Hence, experiments were made to examine the aerodynamic response of the elliptical airfoil model of 18% thickness ratio to a cyclic change in the jet mass flow.

In the experiments, the cyclic change in mass flow was accomplished by the use of a rotating butterfly valve which partially interrupted the flow into the model proper. The cycling of the jet at any specified frequency was achieved by controlling the rotational speed of the valve. During the test, the cyclic pressure inside the model and the corresponding cyclically varying normal and axial forces were measured. The instrumentation for these measurements was discussed in the previous section.

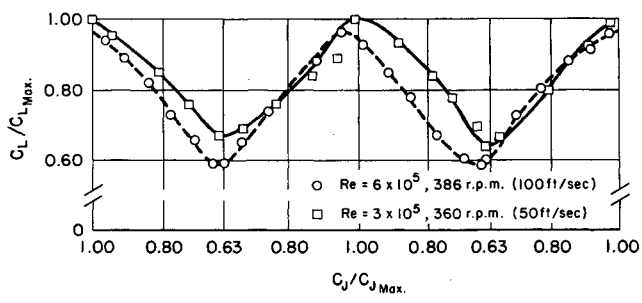

Fig. 14 Pulsating lift coefficient ratio vs pulsating jet coefficient ratio for 18% thickness model.

During the tests, three rotational speeds of the valve were made, namely 360 rpm, 210 rpm, and 150 rpm. These valve speeds correspond to jet mass flow variations of 12, 7, and 5 cps, respectively. A typical four cycles of pulsating lift and the pressure inside the model were obtained from the testing results for the valve speed at 360 rpm. These results are plotted in Fig. 13 as a function of time. It is very interesting to note that the pulsating lift is almost completely in phase with the pulsating pressure inside the model; hence, there exists a negligible delay in the system of pulsating supply pressure, pulsating jet mass flow, and lift.

Figure 14 is a plot of the pulsating lift coefficient ratio vs the pulsating jet coefficient ratio for two different Reynolds numbers. The typical two cycles of pulsating lift coefficient (measured at two different Reynolds numbers) shown are very close. The results of these tests clearly indicate that the periodic variation of lift on the airfoil can be fulfilled by cyclic variation of the jet momentum; hence, the lift control problems reduce to simply the problem of pressure control inside the model.

Response of Chordwise Pressure of the Model to Cyclic Change of Jet

Experiments were made to examine the response of the chordwise static pressure of the elliptical airfoil mode of 12% thickness ratio to a cyclic change in the mass flow. During the tests, two rotational speeds of the valve were used, namely, 300 rpm and 150 rpm, corresponding to the jet mass flow variation of 10 and 5 cps. A typical seven cycles of pulsating static pressure and the pressure inside the model were obtained for valve speed at 300 rpm, and it is shown in Fig. 15 as a function of time. It is noted that there is a time lag of about $\frac{1}{5}$ sec between the pulsating static pressure and the pressure inside the model. The time lag between the pulsating static pressure and the pressure inside the model is attributed to the effects of the tubing length between the static pressure orifices and the pressure transducers.

Conclusions

Experimental results obtained for elliptical airfoils of both 18 and 12% thickness ratio with trailing-edge jets are in good agreement with available theories and other experimental data. Lift forces determined from electric strain-gage data agree very well with those obtained from steady-state pressure measurements. The measured drag data are reasonable but possess more scatter than is desirable; hence, further refinement in the drag force measurement is needed. The pitching moments calculated from the pressure data are reasonable

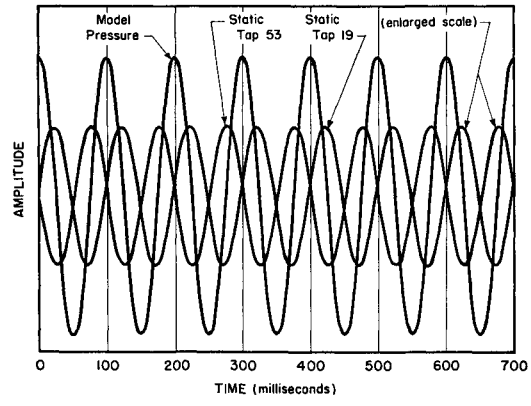

Fig. 15 Pulsating static pressure and model pressure for elliptical airfoil of 12% thickness ratio (valve speed = 300 rpm).

and agree well with the semiempirical expression previously determined.

Most encouraging results were obtained from an experiment performed on the elliptical airfoil of 18% thickness ratio with dual symmetrical jets. These results indicate that the leading-edge jet does not disturb the flow and actually furnishes some additional reaction force to the lift. Hence, the important application of the elliptical airfoil (or oval airfoil) with dual jets to the retreating blade of a helicopter rotor is evident.

Furthermore, the results of aerodynamic response measurements of the model to cyclic changes in the blowing jet are surprisingly encouraging. The cyclic valve was tested at frequencies equivalent to twice that of the rotational speed of a conventional helicopter blade, and the response of the lift was found to be excellent with negligible delay. The response of the drag as well as the chordwise pressure distribution to the cyclic changes in the blowing jet were also found to be very good. These results clearly indicate that the periodic variation of lift on the airfoil can be fulfilled by cyclic variation of the jet momentum; hence, the circulation control problem is reduced to simply the problem of pressure control inside the model.

References

[1] Weber, J., "The Calculation of the Pressure Distribution over the Surface of Two-Dimensional and Swept Wings with Symmetrical Airfoil Sections," R and M 2918, 1956, Aeronautical Research Council.

[2] Küchemann, D., "A Method for Calculating the Pressure Distribution over Jet Flapped Wing," R and M 3036, 1957, Aeronautical Research Council.

[3] Spence, D. A., "The Lift Coefficient of a Thin Jet-Flapped Wing," *Proceedings of the Royal Society*, Series A, Vol. 238, No. 1212, Dec. 1956, pp. 46–48.

[4] Yuan, S. W. et al., "Investigation of Circulation Control Airfoils by Means of Jets," TR 66-72, Nov. 1966, U. S. Army Aviation Materiel Labs., Fort Eustis, Va.

[5] Dimmock, N. A., "Some Future Jet Flap Experiments," Memo M.255, May 1956, National Gas Turbine Establishment.

[6] Davidson, I. M. and Stratford, B. S., "An Introduction to the Jet Flap," Rept. R.155, June 1954, National Gas Turbine Establishment.

SEPT.-OCT. 1970 J. AIRCRAFT VOL. 7, NO. 5

A Review of Para-Foil Applications

JOHN D. NICOLAIDES*

University of Notre Dame, Notre Dame, Ind.

AND

RALPH J. SPEELMAN III†

U.S. Air Force, Wright-Patterson Air Force Base, Ohio

AND

GEORGE L. C. MENARD‡

U.S. Navy, El Centro, Calif.

Numerous tests of various para-foil designs have been carried out by the University of Notre Dame, the U.S. Air Force, the U.S. Navy, the U.S. Army, NASA, and industry. These tests include wind-tunnel studies of models ranging in size from 0.2 to 300 ft² and free-flight tests of units ranging in size from 8 to 864 ft². Unmanned free-flight tests of certain units have included deployment tests to 350 fps, guidance and control tests with payloads to 2000 lb, and glide performance tests with payloads to 2000 lb. Manned jumps and manned ascending flights have been made with units ranging in size from 165 to 360 ft². Manned flights using propeller powered carts have been made with a 360-ft² unit. The various para-foil application programs will be discussed and a summary of results obtained from various wind-tunnel and free-flight tests will be given.

Nomenclature

AR = aspect ratio (AR = span divided by chord), dimensionless
C_L = coefficient of lift, dimensionless
KIAS = knots indicated airspeed
L/D = lift-to-drag ratio, dimensionless
MSL = mean sea level
ND$x.x(yy)$ = Notre Dame para-foil of aspect ratio $x.x$ and area of yy ft² [e.g., an ND 2.0 (90) para-foil has AR = 2, S = area = 90 ft², span = 13.4 ft, and chord = 6.7 ft]
q = dynamic pressure, psf
S = canopy area (S = span times chord)
α = angle of attack of bottom surface of para-foil, deg

Presented as Paper 68-968 at the AIAA 2nd Aerodynamic Deceleration Conference, El Centro, Calif., September 23–25, 1968; submitted December 17, 1968; revision received January 14, 1970.

* Chairman and Professor, Department of Aerospace Engineering. Associate Fellow AIAA.

† Project Engineer, Air Force Flight Dynamics Laboratory.

‡ Project Engineer, Naval Aerospace Recovery Facility. Member AIAA.

Introduction

THE para-foil§ is a true flying wing made entirely of nylon cloth with no rigid members, (Figs. 1, 4–7). Like a rigid wing, it has an upper and a lower surface, and an airfoil section. The leading edge is open to permit inflation by the ram air pressure. The para-foil is composed of numerous cells which give this cloth wing its unique rigid shape.

It is fabricated of a low porosity nylon cloth and can be packed and deployed in a manner similar to a conventional parachute. Pennants are distributed along the bottom surface to which the suspension lines are attached. These pen-

§ The para-foil is a proprietary product (patent 3285546) of Space Recovery Research Center Inc. The University of Notre Dame has a license for research and design of para-foils.